Regulation of Etioplast Pigment-Protein Complexes, Inner Membrane Architecture, and Protochlorophyllide *a* Chemical Heterogeneity by Light-Dependent NADPH:Protochlorophyllide Oxidoreductases A and B[1]

Fabrice Franck, Ulrich Sperling, Geneviève Frick, Babette Pochert, Barbara van Cleve, Klaus Apel, and Gregory A. Armstrong*

Laboratory of Photobiology, Department of Plant Biology, Université de Liege, Liege, Belgium (F.F.); and Institute for Plant Sciences, Plant Genetics, Swiss Federal Institute of Technology, Zurich, Switzerland (U.S., G.F., B.P., B.v.C., K.A., G.A.A.)

The etioplast of dark-grown angiosperms is characterized by the prolamellar body (PLB) inner membrane, the absence of chlorophyll, and the accumulation of divinyl and monovinyl derivatives of protochlorophyll(ide) *a* [Pchl(ide) *a*]. Either of two structurally related, but differentially expressed light-dependent NADPH:Pchlide oxidoreductases (PORs), PORA and PORB, can assemble the PLB and form dark-stable ternary complexes containing enzymatically photoactive Pchlide-F655. Here we have examined in detail whether these polypeptides play redundant roles in etioplast differentiation by manipulating the total POR content and the PORA-to-PORB ratio of etiolated Arabidopsis seedlings using antisense and overexpression approaches. POR content correlates closely with PLB formation, the amounts, spectroscopic properties, and photoreduction kinetics of photoactive Pchlide, the ratio of photoactive Pchlide-F655 to non-photoactive Pchl(ide)-F632, and the ratio of divinyl- to monovinyl-Pchl(ide). This last result defines POR as the first endogenous protein factor demonstrated to influence the chemical heterogeneity of Pchl(ide) in angiosperms. It is intriguing that excitation energy transfer between different spectroscopic forms of Pchl(ide) in etiolated cotyledons remains largely independent of POR content. We therefore propose that the PLB contains a minimal structural unit with defined pigment stoichiometries, within which a small amount of non-photoactive Pchl(ide) transfers excitation energy to a large excess of photoactive Pchlide-F655. In addition, our data suggests that POR may bind not only stoichiometric amounts of photoactive Pchlide, but also substoichiometric amounts of non-photoactive Pchl(ide). We conclude that the typical characteristics of etioplasts are closely related to total POR content, but not obviously to the specific presence of PORA or PORB.

Etioplasts are the typical achlorophyllous plastids found in the cotyledons of dark-grown angiosperm seedlings and are transformed into chloroplasts during light-dependent greening. Two obvious features distinguish etioplasts from other plastid types (for review, see Griffiths, 1991; Ryberg and Sundqvist, 1991): the prolamellar body (PLB), a highly regular, lattice-like membrane structure composed of interconnected tubules, and the accumulation of the chlorophyll (Chl) precursor, protochlorophyll(ide) *a* [Pchl(ide) *a*] (Scheumann et al., 1999). PLB formation and the accumulation of Pchl(ide) correlate with the presence of the strictly light-dependent NADPH:protochlorophyllide (Pchlide) oxidoreductase (POR; EC 1.3.1.33), a nuclear-encoded enzyme that is synthesized as a cytosolic precursor and imported into plastids (Griffiths, 1978, 1991; Apel et al., 1980). POR is the most abundant protein of the PLB and is also present in small amounts in the unstacked stromal prothylakoid (PT) membranes (Ryberg and Sundqvist, 1982, 1991). This enzyme catalyzes the only light-dependent reaction in the Chl biosynthetic pathway and is hence intimately involved in the greening of angiosperms (for review, see Beale, 1999). Dark-stable Pchlide:NADPH:POR ternary complexes are poised such that photon absorption by the pigment leads to its immediate reduction. The chlorophyllide *a* (Chlide *a*) product is subsequently converted to the esterified pigments Chl *a* and Chl *b* in conjunction with the dispersal of the PLB and the formation of functional photosynthetic membranes (Ryberg and Sundqvist, 1991). POR is thus a plastid-specific photon sensor that triggers light-dependent Chl biosynthesis and membrane reorganization during the transformation of etioplasts to chloroplasts.

Several factors that reflect the natural complexity of angiosperms complicate analyses of etioplast differentiation and chloroplast formation, however. First, the Pchl(ide) *a* present in vivo is actually a chemically heterogeneous mixture of pigments dominated by unesterified divinyl (DV)- and monovinyl (MV)-Pchlide, but that also includes a small amount

[1] This work was supported by the Belgian Nation Funds of Scientific Research (grant nos. FRFC 2.4523.95 and 2.4597.99), by the Swiss Federal Institute of Technology Zurich, and by the Swiss National Science Foundation Swiss Priority Programme Biotechnology.

* Corresponding author; e-mail gregory.armstrong@ipw.biol.ethz.ch; fax 41–1–632–1081.

of esterified protochlorophyll (Pchl; Belanger and Rebeiz, 1980; Carey and Rebeiz, 1985; Shioi and Takamiya, 1992; Whyte and Griffiths, 1993; Ioannides et al., 1994). In contrast to Pchlide, Pchl seems neither to be a POR substrate nor to bind to the enzyme (Schoch et al., 1995; Ouazzani Chahdi et al., 1998; Klement et al., 1999).

Second, etiolated cotyledons contain several spectroscopically distinct Pchl(ide) species that can be observed in situ (for review, see Virgin, 1981; Ryberg and Sundqvist, 1991). Photoactive Pchlide, i.e. the pigment fraction bound in POR ternary complexes that is immediately reduced to Chlide upon illumination, exhibits room temperature absorption maxima at about 640 and 650 nm (Pchlide-A640 and Pchlide-A650, respectively). These pigment forms give rise to low temperature (77 K) fluorescence emission maxima at 645 and 655 nm (Pchlide-F645 and Pchlide-F655, respectively). Only photoactive Pchlide-F655 is readily observed, however, due to efficient energy migration from Pchlide-A640 to Pchlide-A650 (Kahn et al., 1970; Böddi et al., 1992). Photoactive Pchlide-F655 is the dominant pigment form in PLBs, which have a 10-fold higher Pchl(ide) content than the PTs (Ryberg and Sundqvist, 1982; Böddi et al., 1989; Ouazzani Chahdi et al., 1998). Pchlide-F655 seems to arise from highly aggregated POR ternary complexes, whereas Pchlide-F645 may represent a smaller aggregate at the periphery of the PLB or in the PTs (Böddi et al., 1989; Ryberg et al., 1992; Ouazzani Chahdi et al., 1998). Non-photoactive Pchl(ide), i.e. the pigment fraction that is not immediately reduced to Chlide by a saturating light flash, consists of a poorly defined mixture of Pchlide and Pchl pigments that is highly enriched in the PTs (Ryberg and Sundqvist, 1982; Böddi et al., 1989). Non-photoactive Pchl(ide) displays room temperature absorption and low temperature fluorescence emission maxima at 628 nm [Pchl(ide)-A628] and 632 nm [Pchl(ide)-F632], respectively (Ryberg and Sundqvist, 1991), but is actually spectroscopically heterogeneous (Cohen and Rebeiz, 1981; Schoefs and Franck, 1998).

Third, two differentially regulated genes, *PORA* and *PORB*, that encode structurally related light-dependent POR enzymes have been identified in Arabidopsis and barley (Armstrong et al., 1995; Holtorf et al., 1995a). *PORA* is strongly expressed in etiolated seedlings and the abundance of its mRNA is dramatically down-regulated by light. *PORB* is also expressed in etiolated tissues, but its mRNA is less strongly down-regulated by light than *PORA* in Arabidopsis or is even constitutively expressed during greening in barley. The amount of *PORA* mRNA is much higher than that of *PORB* mRNA in etiolated barley, although the two mRNAs accumulate to similar levels in etiolated Arabidopsis.

Because the relationships between the various chemically and spectroscopically distinct Pchl(ide) species, their associations with the PORA and PORB enzymes, and the intraplastidic localization of the different pigments and pigment-protein complexes remain largely undefined, it is not yet possible to present an integrated model describing the etioplast. In this context, the question of whether the two angiosperm POR enzymes perform unique or redundant functions has been the subject of vigorous in vivo investigation in Arabidopsis (Lebedev et al., 1995; Runge et al., 1996; Sperling et al., 1997, 1998, 1999) and in vitro experimentation using barley PORA and PORB (Reinbothe et al., 1996, 1999). On the one hand, PORA has been suggested to be specifically involved in photoactive Pchlide-F655 formation, in the assembly of the PLB, and in protection against non-photoactive Pchl(ide)-F632-induced photooxidative damage (Lebedev et al., 1995; Reinbothe et al., 1996). On the other hand, constitutive overexpression of the Arabidopsis POR enzymes in the homologous host demonstrates that not only PORA, but also PORB can independently perform all of these functions (Runge et al., 1996; Sperling et al., 1997, 1998, 1999). It has recently been speculated that etiolated barley seedlings contain a supercomplex composed of non-photoactive protochlorophyll(ide) *b* [Pchl(ide) *b*]:NADPH:PORA and photoactive Pchlide *a*:NADPH:PORB ternary complexes in a 5:1 ratio (Reinbothe et al., 1999). This supercomplex is hypothesized to assemble the PLB, provide light harvesting and photoprotective functions during greening, and allow the selective reduction of Pchlide *a* bound to PORB. However, this model conflicts with other published data (i.e. Sperling et al., 1998; Klement et al., 1999; Scheumann et al., 1999) and is problematic for a number of reasons detailed elsewhere (for review, see Armstrong et al., 2000).

Here we have studied the roles of PORA and PORB in etioplast differentiation by comparing the plastid inner membrane structures, the distribution and in situ spectroscopic properties of Pchl(ide) pigments and pigment-protein complexes, and the chemical heterogeneity of Pchl(ide) in POR-antisense and POR-overexpressing Arabidopsis seedlings. The goal of these experiments has been to rigorously investigate whether PORA and PORB perform unique or redundant functions in etioplasts and how their levels influence the development of this plastid type.

RESULTS

Inhibition of Expression of *PORA* and *PORB* in Etiolated Arabidopsis Seedlings

Agrobacterium tumefaciens-mediated transformation of Arabidopsis root explants led to the isolation of putative transgenic lines expected to constitutively express Arabidopsis *PORA* or *PORB* antisense mRNA. An initial survey of the *POR* sense mRNA levels by gel-blot analysis was conducted using etiolated seedlings of all antisense lines available in the homozygous state. On the basis of these results, two lines each

carrying *PORA*-antisense (PAA) or *PORB*-antisense (PBA) transgenes were selected to examine the quantitative inhibition of *POR* gene expression by the antisense constructs and the specificity of this inhibition for *PORA* and *PORB*.

POR mRNA and POR protein levels were determined in etiolated seedlings, as shown in Figure 1. The decrease in the endogenous *POR* mRNA levels relative to the wild type varied between 2- and 10-fold, with lines PBA-24 and PBA-25 displaying the strongest antisense effects (Fig. 1A). By measuring *PORA* and *PORB* mRNA levels individually in the same experiment it was possible to demonstrate that either *POR*-antisense transgene equally inhibited the expression of both endogenous *POR* genes. In this context we note that the two *POR* cDNA sequences used in the antisense constructs were 83% identical (Armstrong et al., 1995).

The total POR contents of seedlings harvested in parallel to those used for the RNA analysis were determined immunologically following electrophoretic separation of total protein extracts by SDS-PAGE and subsequent gel blotting. PORA and PORB comigrate and are detected as a single immunoreactive signal with an apparent molecular mass of about 36 kD (Fig. 1B). In antisense lines PAA-28, PBA-24, and PBA-25 the total POR content was reduced 2- to 3-fold relative to the wild type, a significant decrease given that POR is by far the most abundant protein in the PLB (Ryberg and Sundqvist, 1991). Because neither antisense construct specifically inhibited the accumulation of a particular *POR* mRNA, it is likely that all four PAA and PBA lines contain decreased levels of both POR enzymes.

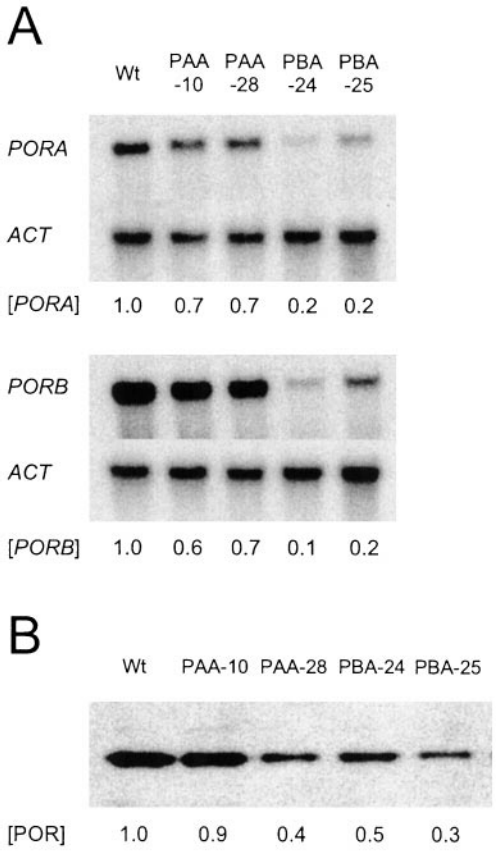

Figure 1. *POR* mRNA and POR protein amounts in etiolated Arabidopsis POR-antisense seedlings. A, *PORA* and *PORB* mRNA levels in transgenic PAA and PBA lines. Gel blots were prepared with 5 μg of total RNA from 4-d-old seedlings and were probed for the mRNAs indicated at the left. *ACT* mRNA provides a control for the sample loading. Numbers at the bottom represent the *ACT*-corrected amounts of the relevant mRNAs from transgenic seedlings, relative to the wild-type (Wt) control. B, Total POR protein levels. A gel blot was prepared using 5 μg of total protein from extracts of 4-d-old seedlings that, independent of genotype, contained similar amounts of total protein on a per seedling basis. Numbers at the bottom represent the amounts of immunoreactive POR protein detected relative to the wild-type control.

Determination of Etioplast Membrane Ultrastructure and the Distribution of Pchl(ide) Pigment Forms

Ultrathin sections of cotyledon cells from etiolated seedlings of various genotypes were viewed by transmission electron microscopy. For this analysis we selected the POR-antisense lines PAA-28 and PBA-24 and the PORB-overexpressing line PBO-10, which accumulates about twice as much total POR as the wild type under these conditions (Sperling et al., 1998). As seen in Figure 2, a wide range of plastid inner membrane architectures were observed, depending upon the seedling genotype. Sections of wild-type etioplasts revealed a PLB from which unstacked PTs protruded into the stroma in 76% of the 45 plastids examined (Fig. 2A). PBO-10 etioplasts consistently displayed very extensive PLBs (Fig. 2B). Unusually large, albeit less extensively developed PLBs have also been observed in the PORA- or PORB-overexpressing lines PAO-3 and PBO-1, respectively (Sperling et al., 1998). PBO-10 etioplasts were also irregular in shape, in contrast to the spherical or ellipsoidal plastids found in cotyledons of the other seedling genotypes (Fig. 2, A and C–F), and tended to be larger than those of the wild type.

In line PAA-28, PLBs and PTs that resembled those seen in the wild type were visible in 41% of the 49 etioplasts examined (Fig. 2C), whereas only PTs were observed in the remaining plastids (Fig. 2D). PAA-28 etioplasts were usually slightly smaller than those of the wild type. In line PBA-24, a PLB was visible in 50% of the 112 etioplasts viewed (Fig. 2, E and F). In striking contrast to seedlings of other genotypes, concentric rings of PTs were common in PBA-24 plastids. Etioplasts of this line were, in general, somewhat larger than those of the wild type.

Low-temperature fluorescence spectroscopy was performed on intact cotyledons of lines PAA-28, PBA-

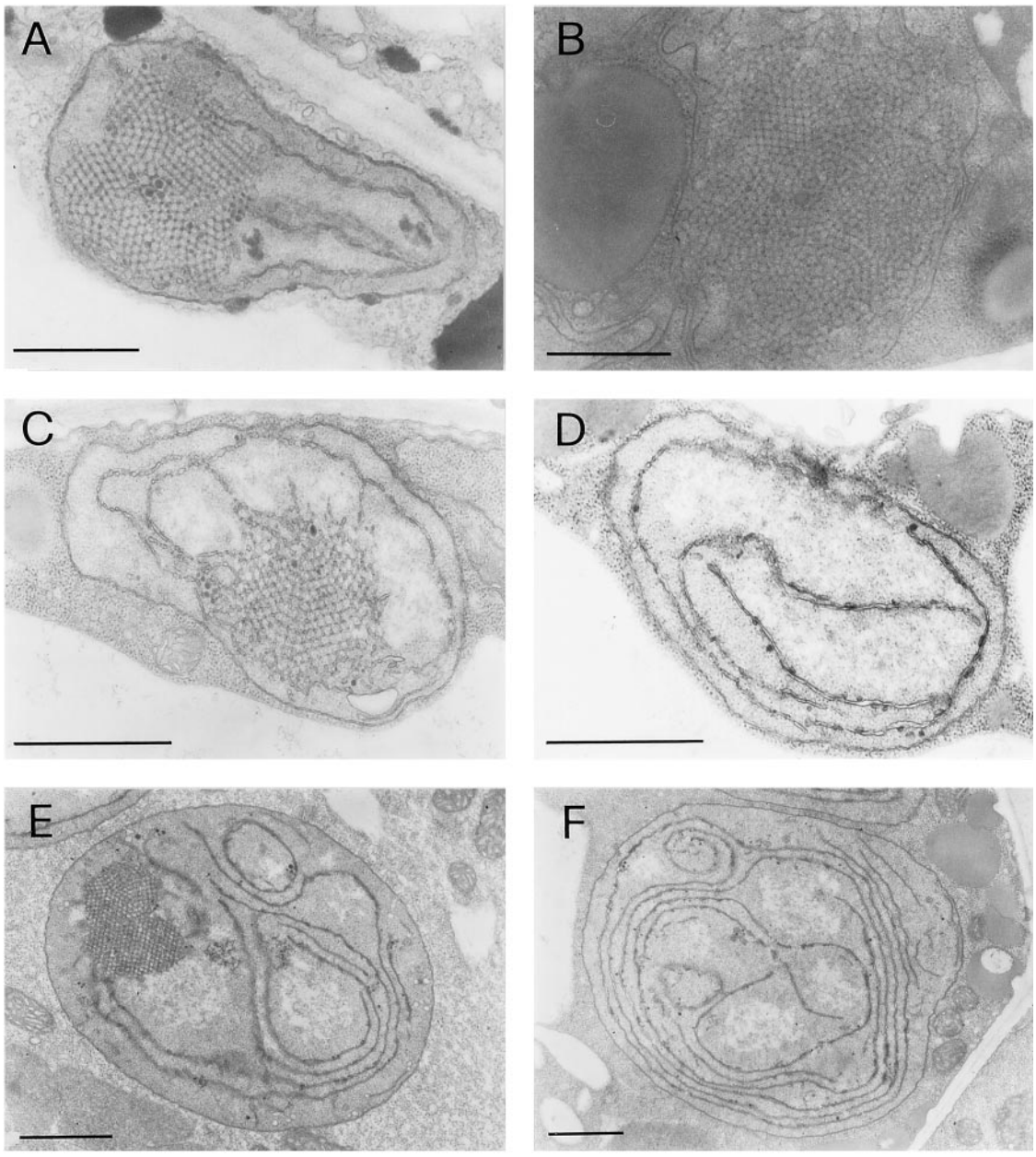

Figure 2. Etioplast ultrastructure in POR-antisense and POR-overexpressing seedlings. A, Wild type. B, Line PBO-10 (strong PORB overexpression). C, Line PAA-28 (weak POR antisense) with PLB. D, Line PAA-28 without PLB. E, Line PBA-24 (strong POR antisense) with PLB. F, Line PBA-24 without PLB. Membrane ultrastructure of cotyledon plastids from 4-d-old seedlings was examined by transmission electron microscopy. Magnifications were 20,000× for A and B; 25,000× for C and D;, 15,000× for E; and 12,000× for F. Bars in A through F = 1 μm.

24, and PBO-10 to obtain qualitative data on the pigments and pigment-protein complexes present in situ. As illustrated in Figure 3, etiolated wild-type cotyledons contained pigment forms corresponding to Pchl(ide)-F632, emitting in this case at 633 nm, and Pchlide-F655. A single 1-ms light flash supplied at −20°C reduced virtually all of the accumulated Pchlide-F655 to a pigment form emitting at 688 nm (Fig. 3A) that corresponds to Chlide-F690, the first long-lived photoreduction product (Sironval and Brouers, 1970). The pre- and post-flash emission spectra of the line PAA-28 were similar to those of the wild type (Fig. 3B). Dramatic effects on the content of Pchl(ide) pigment forms prior to the flash treatment were, however, observed in lines PBA-24 and PBO-10 (Fig. 3, C and D). Line PBA-24 contained a much higher ratio of non-photoactive Pchl(ide)-F632-to-photoactive Pchlide-F655 than was found in the wild type. In line PBO-10 exactly the opposite effect was observed, in qualitative agreement with less extreme changes in the

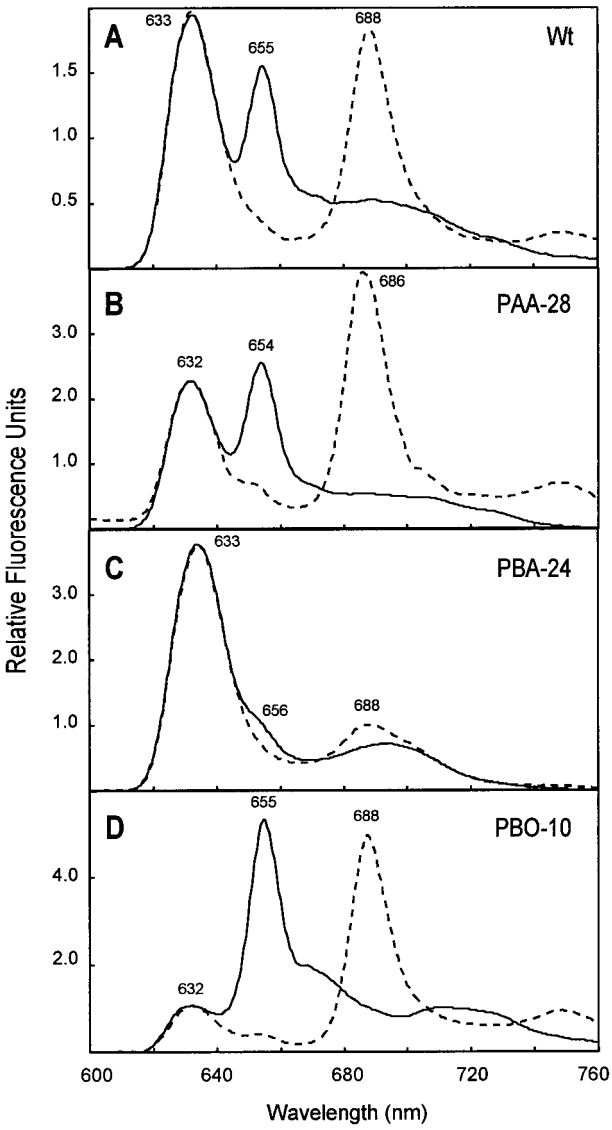

Figure 3. Fluorescence emission spectra of Pchl(ide) pigment forms present in situ in etiolated POR-antisense and POR-overexpressing seedlings. A, Wild type. B, Line PAA-28 (weak POR antisense). C, Line PBA-24 (strong POR antisense). D, Line PBO-10 (strong PORB overexpression). In situ low temperature fluorescence spectra of unilluminated (solid curves) and flash-illuminated (dashed curves) cotyledons of 4-d-old seedlings. Emission bands observed with an excitation wavelength of 440 nm include non-photoactive Pchl(ide)-F632, photoactive Pchlide-F655 arising from the aggregated Pchlide:NADPH:POR ternary complex, and, after flash treatment applied at −20°C, Chlide-F690. The broad pre-flash fluorescence emissions centered at about 693 nm in PBA-24 cotyledons (C) and roughly 720 nm in PBO-10 cotyledons (D) represent vibrational sublevels of Pchl(ide)-F632 and Pchlide-F655, respectively (Böddi et al., 1992).

ratio of pigment forms previously reported for lines PAO-3 and PBO-1 (Sperling et al., 1998).

To obtain information about the absolute amounts of different Pchl(ide) pigment forms present in cotyledons of etiolated seedlings, room temperature fluorimetric measurements of acetone-extracted pigments were performed. Figure 4 illustrates that the amounts of total Pchl(ide) and photoactive Pchlide are lower in the POR-antisense lines and higher in the POR-overexpressing lines than in the wild type. The total Pchl(ide) content as a percentage of the wild-type value ranged from about 60% in line PAA-28 to 210% in line PBO-10 (Fig. 4A). The comparable photoactive Pchlide contents of seedlings of these lines were 60% and 260%, respectively (Fig. 4B). With respect to the ratios of different pigment forms (Fig. 4C), the wild type contained about 2-fold more photoactive than non-photoactive pigment (0.77 versus 0.40 ng/cotyledon pair). Lines PAA-28, PAO-3, PBO-1, and PBO-10 displayed pigment ratios that ranged from about 2.1 to 4.8. Therefore, in seedlings of these genotypes, total Pchl(ide) consists mostly of photoactive Pchlide. It is exceptional that the ratio of photoactive to non-photoactive pigment was only 0.9 in the strong POR-antisense line PBA-24.

The Relationship between the Amounts of Photoactive Pchlide and Total POR in Etiolated Cotyledons

To determine whether photoactive Pchlide and total POR protein always occur in a defined stoichiometry in vivo, a plot of the relative amounts of total POR protein (Fig. 1B; Sperling et al., 1998) versus photoactive Pchlide (Fig. 4B) in POR-antisense, wild-type, and POR-overexpressing seedlings was prepared. As seen in Figure 5, this analysis clearly indicates a direct proportionality between the amounts of photoactive Pchlide in cotyledons and total POR protein in seedlings, most of which is found in cotyledons, over the 6-fold range of POR expression levels available in vivo. The high correlation coefficient between the data points, including those derived from seedlings that specifically overexpress either PORA or PORB, also seems to exclude the possibility that photoactive Pchlide content depends upon the PORA-to-PORB ratio.

Perturbation of the Spectroscopic Properties of Photoactive Pchlide as a Function of POR Content

The spectroscopic properties of photoactive Pchlide and the interactions between Pchl(ide) pigment forms were further examined by recording in situ low temperature excitation spectra of the fluorescence emitted by Pchlide-F655 upon excitation with different wavelengths of light from the Soret (blue) region. Some of these data are presented in Figure 6A for the transgenic lines PBA-24 and PBO-10, whose ratios of photoactive-to-non-photoactive pigment deviated most strongly from that of the wild type (Fig. 4C). In cotyledons of wild-type seedlings, Pchlide-F655 showed a main excitation band at 445 nm and two shoulders at 459 and 472 nm whose wavelength values were obtained from fourth-derivative analysis of the spectra (data not shown). These shoulders were

very weak in line PBA-24, whereas in line PBO-10 their relative amplitudes were enhanced to such an extent that the excitation maximum was shifted to 459 nm. The excitation spectra of non-photoactive

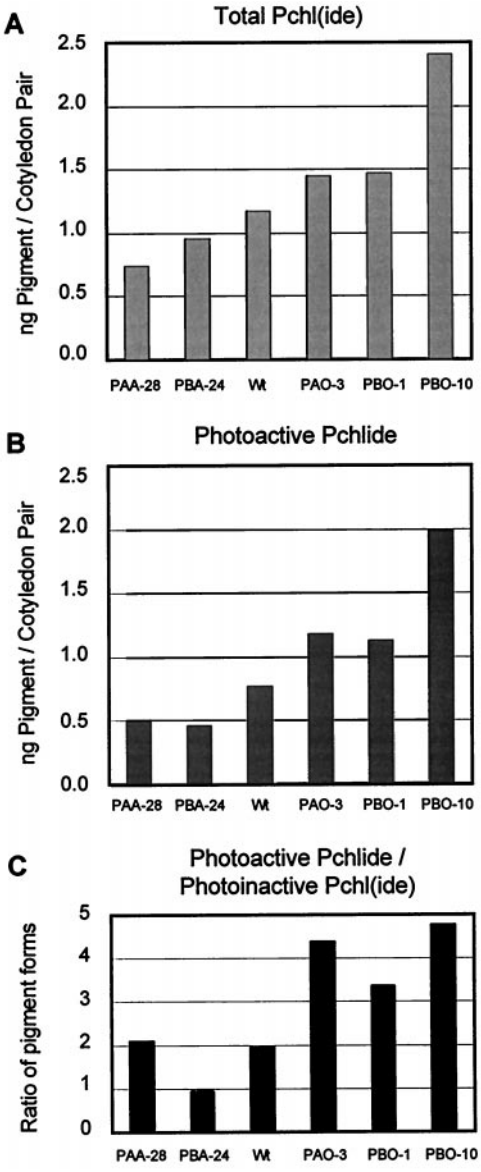

Figure 4. Quantitative determination of Pchl(ide) pigment forms present in etiolated seedlings. A, Total Pchl(ide). B, Photoactive Pchlide. C, Ratio of photoactive Pchlide-to-non-photoactive Pchl(ide). Room temperature fluorescence emission measurements of the acetone-extracted total pigments from unilluminated and flash-illuminated cotyledons of 4-d-old wild-type, POR-antisense, and POR-overexpressing seedlings collected at an excitation wavelength of 435 nm. Total Pchl(ide) was calculated from the pre-flash fluorescence emission band at 634 nm. Photoactive Pchlide-F655 was determined based on the post-flash emission at 672 nm that results from its quantitative POR-mediated reduction to Chlide. Non-photoactive Pchl(ide)-F632 was set equal to the difference between these two quantities. Pigment amounts are given on a per cotyledon pair basis. Seedling genotypes are given from left to right in the order of increasing total POR content (see Fig. 5).

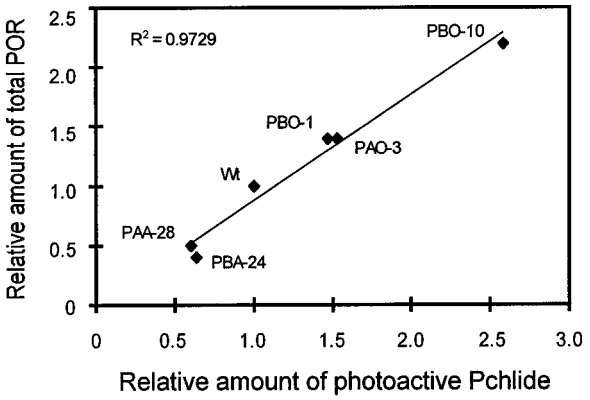

Figure 5. Quantitative correlation analysis of the amounts of total POR protein and photoactive Pchlide in etiolated seedlings. The ratio of total POR protein in seedlings-to-photoactive Pchlide in cotyledons calculated for 4-d-old seedlings of each transgenic genotype relative to the wild type. A best-fit trendline through the data points was calculated and its correlation coefficient determined.

Pchl(ide)-F632 displayed a maximum at 442 nm in wild-type cotyledons and showed relatively minor genotype-specific variations (Fig. 6B).

As illustrated in Figure 7, the ratio of the 655 nm fluorescence intensities upon excitation with 465 versus 440 nm light ($I_{F655,\ 465}/I_{F655,E440}$) was taken as an index of the relative contributions of the 459 and 472 nm components versus the 445 nm component to the excitation spectra of Pchlide-F655. This ratio was about 0.65 in the wild type and in lines PAA-28, PAO-3, and PBO-1. In seedlings of these four genotypes the Soret region excitation spectra of Pchlide-F655 showed relatively small differences (Fig. 6A and data not shown). Line PBO-1 has a total POR content similar to that of line PAO-3 and was included in the analysis to allow a more direct comparison of the effects of PORA versus PORB overexpression. The similarity between the $I_{F655,465}/I_{F655,E440}$ ratios and excitation spectra of Pchlide-F655 in these two lines indeed reinforces the conclusion based on the in situ low temperature emission spectra (Fig. 3; Sperling et al., 1998) that the PORA-to-PORB ratio does not significantly influence the spectroscopic properties of photoactive Pchlide.

On the other hand, lines PBA-24 and PBO-10, whose Pchlide-F655 excitation spectra deviated significantly from that of the wild type (Fig. 6), displayed $I_{F655,465}/I_{F655,E440}$ ratios of 0.35 and 0.94, respectively (Fig. 7). To test whether these deviations were caused by genotype-specific differences in the screening efficiency of carotenoids in the Soret region, seedlings were treated with norflurazon, an inhibitor of carotenoid biosynthesis (Kümmel and Grimme, 1974). This treatment caused a 10-fold decrease in the amount of colored carotenoids, but did not affect the excitation spectra in a manner consistent with genotype-specific differences in carotenoid screening (data not shown). In line PBA-24 we also verified that the smaller contributions of the 459 and

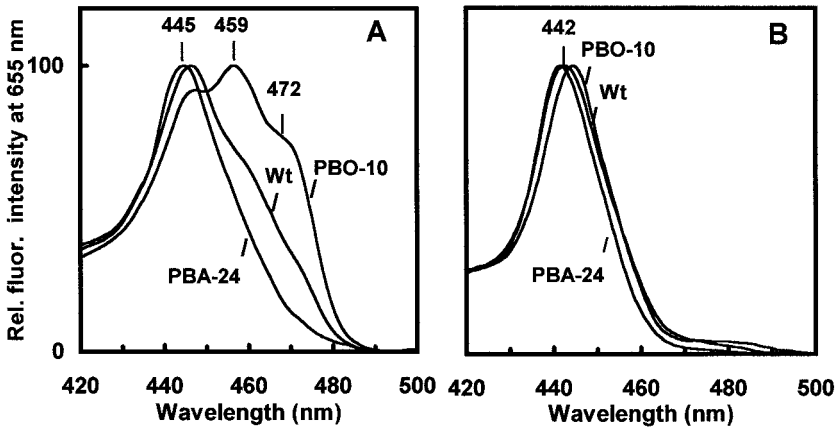

Figure 6. Fluorescence excitation spectra from the Soret region of Pchl(ide) pigment forms present in situ in etiolated seedlings. A, Photoactive Pchlide-F655. B, Non-photoactive Pchl(ide)-F632. In situ low temperature fluorescence spectra normalized at their respective maxima from cotyledons of 4-d-old wild-type, POR-antisense, and POR-overexpressing seedlings. Seedling genotypes are given and the wavelengths positions of the maxima and a shoulder are indicated.

472 nm bands and hence the larger relative contribution of the 445 nm band to the emission at 655 nm did not simply reflect a larger direct contribution of non-photoactive Pchl(ide)-F632. In this analysis the experimental Pchlide-F655 excitation spectrum (Fig. 6A) was corrected by subtraction of the small contribution of Pchl(ide)-F632 and hence its excitation spectrum, to the emission band at 655 nm (data not shown).

POR Dependence of the Chemical Heterogeneity of Pchl(ide) *a* in Etiolated Seedlings

To further investigate the genotype-specific differences in the in situ excitation spectra of photoactive Pchlide-F655 (Fig. 6A) we examined whether the Pchl(ide) pool of etiolated Arabidopsis seedlings might be chemically heterogeneous. For this purpose, the spectroscopic properties of organically extracted pigments from cotyledons of etiolated Arabidopsis seedlings were analyzed in detail. The room temperature fluorescence emission spectra of acetone-extracted total Pchl(ide) and, subsequent to flash illumination, of non-photoactive Pchl(ide) displayed maxima at 634 nm upon excitation at 435 nm for seedlings of all genotypes (data not shown). Furthermore, as illustrated in Figure 8A for the wild type, the pre- and post-flash Soret excitation spectra of this emission band were virtually identical. If, as proposed for barley, Pchl(ide) *a* and Pchl(ide) *b* had been present in etiolated seedlings and the ratio of their amounts had changed due to the selective reduction of photoactive Pchlide *a* by flash illumination (Reinbothe et al., 1999), one would have expected to find differences in the excitation spectra of the two Pchl(ide) extracts in the Soret region (Schoch et al., 1995).

The low-temperature emission and Soret excitation spectra of acetone-extracted total Pchl(ide) from etiolated wild-type and PBO-10 cotyledons were also collected (data not shown). In these samples the Pchl(ide) emission band was always found at 631 nm, independent of whether the pigments were excited at 440 or 455 nm. At an excitation wavelength of 463 nm almost no fluorescence at 631 nm or at any other wavelength could be detected. Thus no spectroscopic evidence for the existence of Pchl(ide) *b* in etiolated Arabidopsis seedlings could be obtained.

Spectra of pigments from POR-overexpressing seedlings did, however, display small, but reproducible red shifts relative to the wild type in the room temperature excitation maxima of the 634 nm fluorescence emission band arising from acetone-extracted total Pchl(ide) *a* (Fig. 8B and data not shown). The largest effect was seen in line PBO-10 in which the excitation maximum was shifted from 434 to 437.5 nm. These red shifts were observed in the pre- and post-flash excitation spectra of the Pchl(ide) emission (data not shown). We therefore investigated the possibility that etiolated Arabidopsis seedlings might contain a mixture of DV-Pchl(ide) *a* and MV-Pchl(ide) *a* by analogy to other angiosperms (Shioi and Takamiya, 1992; Whyte and Griffiths, 1993; Ioannides et al., 1994), and that differences in the ratio

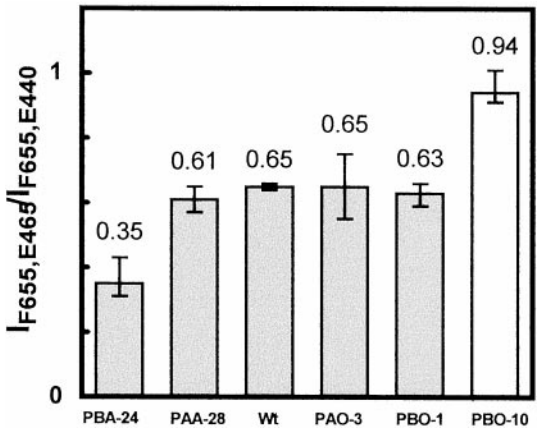

Figure 7. Relative efficiency of the excitation of photoactive Pchlide-F655 by 465 nm light in etiolated seedlings. Calculation of the ratio of the in situ low temperature fluorescence emissions at 655 nm in cotyledons of 4-d-old wild-type and transgenic seedlings upon excitation at 465 or 440 nm. Seedling genotypes are arranged left to right as POR-antisense, wild type, and PORA- or PORB-overexpressing. Error bars indicate the standard deviations.

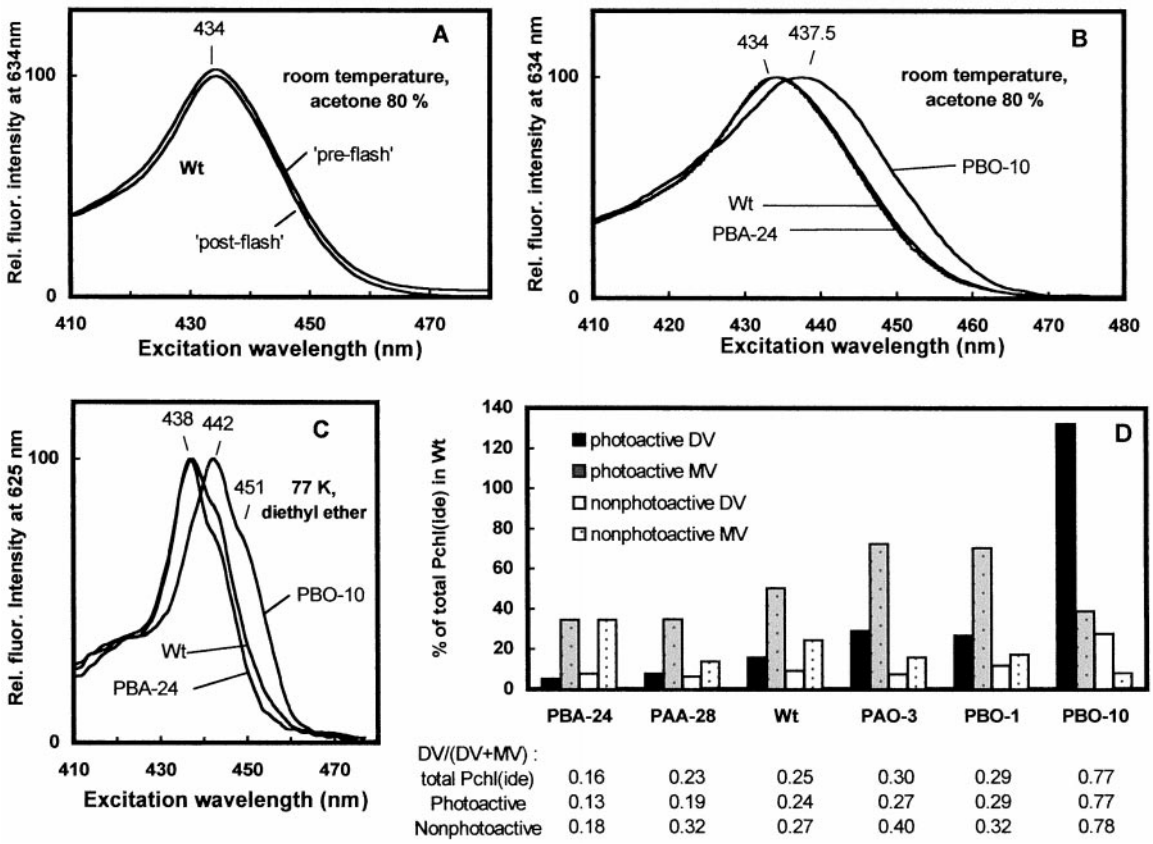

Figure 8. Quantitative determination of the distribution of DV- and MV-Pchl(ide) within the non-photoactive and photoactive pigment fractions of etiolated seedlings. Fluorimetric analysis of the total Pchl(ide) organically extracted from cotyledons of 4-d-old etiolated wild-type, POR-antisense, and POR-overexpressing seedlings. A, Room temperature fluorescence excitation spectra of the Pchl(ide) emission band at 634 nm in acetone-extracted total pigments from unilluminated (solid curves) and flash-illuminated (dashed curves) cotyledons of wild-type seedlings. The spectra were normalized at their respective maxima (434 nm), but have been slightly vertically offset to facilitate their presentation. B, Room temperature fluorescence excitation spectra of the Pchl(ide) emission band at 634 nm in acetone-extracted total pigments from etiolated cotyledons of wild-type, POR-antisense, and POR-overexpressing seedlings. The spectra were normalized at their respective maxima. Seedlings genotypes are given and wavelength positions of the maxima are indicated. C, Low temperature fluorescence excitation spectra of the Pchl(ide) emission band at 625 nm in acetone-extracted total pigments transferred to diethyl ether. The spectra were collected from extracts of etiolated cotyledons of wild-type, POR-antisense, and POR-overexpressing seedlings and were normalized at their respective maxima. Seedling genotypes are given and the wavelength positions of the emission maxima and a shoulder are indicated. D, Determination of the relative amounts of DV- and MV-Pchl(ide) within the photoactive and non-photoactive pigment fractions of the total Pchl(ide) extracted from etiolated cotyledons of wild-type and transgenic seedlings. Pigment amounts are given relative to the wild type for which total Pchl(ide) has been defined as 100%. The respective DV-to-MV pigment ratios for the total Pchl(ide), photoactive Pchlide, and non-photoactive Pchl(ide) fractions of seedlings of each genotype are given below. Seedling genotypes are arranged left to right as POR antisense, wild type, and PORA or PORB overexpressing.

of these pigments might lead to the genotype-specific spectral shifts. For this purpose the acetone-extracted pigments were transferred to diethyl ether and their low temperature excitation spectra were collected to more readily detect differences in the maxima of the Soret region (Tripathy and Rebeiz, 1985).

As seen in Figure 8C, the low temperature excitation spectrum of extracted total Pchl(ide) from the wild type contained a main band at about 438 nm that was slightly blue-shifted to 437 nm or red-shifted to 442 nm in the transgenic lines PBA-24 and PBO-10, respectively. These spectral shifts paralleled those initially observed in cotyledons of seedlings of the same genotypes in the in situ low temperature excitation spectra of Pchlide-F655 (Fig. 6A) and, to a lesser extent, in the room temperature excitation spectra of acetone-extracted total Pchl(ide) (Fig. 8B). The positions of the low temperature excitation maxima and shoulders (Fig. 8C) were consistent with the presence of a mixture of DV- and MV-Pchl(ide) (Tripathy and Rebeiz, 1985; Suzuki and Bauer, 1995) in which the proportion of DV-Pchl(ide) increased as a function of the total POR content in seedlings of different genotypes. By comparing the pre- and post-flash excitation spectra of

the Pchl(ide) emission band at 625 nm in diethyl ether and using a previously described set of equations (Tripathy and Rebeiz, 1985), the relative amounts of the DV- and MV-Pchl(ide) species within the total and non-photoactive Pchl(ide) fractions were determined. These data were combined with the quantitative room temperature analysis of the acetone-extracted pigments (Fig. 4) to calculate the absolute amounts of DV- and MV-Pchl(ide) and the proportions of DV-Pchl(ide) in the photoactive, non-photoactive, and total pigment pools for cotyledons of etiolated seedlings of each genotype (Fig. 8D). DV-Pchl(ide) was found to constitute about 25% of the total Pchl(ide) present in wild-type seedlings. This amount ranged from 16% in PBA-24 seedlings to 77% in PBO-10 seedlings. Lines PBO-1 and PAO-3 contained about the same proportion of total DV-Pchl(ide), indicating that the DV-Pchl(ide)-to-MV-Pchl(ide) ratio was not a specific function of the amount of PORA or PORB, but rather of total POR content (Fig. 5). It is interesting that the POR-dependent perturbation in the ratio of DV-Pchl(ide)-to-MV-Pchl(ide) occurred to roughly similar extents in the photoactive and non-photoactive pigment fractions (Fig. 8D; see "Discussion"). We conclude that genotype-specific differences in the relative amounts of DV- and MV-Pchlide *a* most likely contribute to the perturbations observed in the in situ excitation spectra of Pchlide-F655 in etiolated cotyledons containing drastically altered amounts of POR (Fig. 6A).

Energy Transfer between Different Pchl(ide) Pigment Forms in the PLB

The possibility that the spectral shifts in the low temperature excitation spectra of Pchlide-F655 in PBO-10 and PBA-24 seedlings might arise from differences in excitation energy migration among the various Pchl(ide) forms was also investigated. Such differences could, in turn, reflect fundamental changes in the organization of pigments and pigment-protein complexes within etioplast inner membranes. Energy migration from photoactive Pchlide-F645 and non-photoactive Pchl(ide)-F632 to photoactive Pchlide-F655 has been previously demonstrated (Kahn et al., 1970; Sironval and Brouers, 1970; Ignatov et al., 1983). However, a reliable determination of the relative contributions of different Pchl(ide) forms to the excitation spectrum of Pchlide-F655 in the Soret region is difficult because each pigment form should have two overlapping Soret excitation bands corresponding to the B_x and B_y transitions. When non-photoactive Pchl(ide) and photoactive Pchlide forms simultaneously contribute to the excitation spectrum, the Soret bands of an individual pigment species cannot be conclusively identified. Previous studies have indicated, however, that the excitation shoulder at 460 nm is specific to Pchlide-F655, whereas overlapping bands at shorter wavelengths arise, at least in part, from the other Pchl(ide) forms that transfer excitation energy to Pchlide-F655 (Fradkin et al., 1969; Cohen and Rebeiz, 1981; Ignatov et al., 1983; Böddi et al., 1993).

To investigate energy migration processes we measured the low temperature fluorescence emission arising from Pchlide-F655 upon excitation with different wavelengths of red light. As seen in Figure 9, an excitation maximum at 650 nm and two shoulders at about 628 and 640 nm were visible in the spectra from cotyledons of seedlings of all genotypes (Fig. 9A and data not shown). The components at 628, 640, and 650 nm correspond to the red excitation bands of Pchl(ide)-F632, Pchlide-F645, and Pchlide-F655, respectively, that are always found in the low temperature absorbance spectra of etiolated leaves (Virgin, 1981; Ignatov et al., 1983). These maxima should be insensitive to the chemical heterogeneity of Pchl(ide) because MV- and DV-pigment species display very similar red absorption bands in solution (Shioi and Takamiya, 1992; Knaust et al., 1993). The Pchlide-F655 excitation spectra, illustrated by that of the wild type, could be deconvoluted with less than 1% error using three gaussian components at 628.0 $\pm$ 0.5, 640.4 $\pm$ 0.3, and 651.6 $\pm$ 0.4 nm (one-half-bandwidths of 20.8 $\pm$ 0.7, 15.5 $\pm$ 0.4, 11.8 $\pm$ 0.3 nm, respectively; Fig. 9B and data not shown). The relative amplitudes of the 628, 640, and 652 components and hence the energy migration fluxes from Pchl(ide)-F632 and Pchlide-F645 to Pchlide-F655, were with one exception, very similar in cotyledons of seedlings of all genotypes (Fig. 9C). This result is remarkable because overexpression or antisense manipulation of POR levels can lead to substantial differences in the absolute amount of photoactive Pchlide and the ratios of different Pchl(ide) pigment forms (Figs. 3 and 4). Only in cotyledons of line PBA-24, which has the lowest ratio of photoactive Pchlide-to-non-photoactive Pchl(ide), were the relative amplitudes of the 628 and 640 nm components significantly higher than in the wild type. We therefore cannot exclude the possibility that normal energy transfer processes may be enhanced in seedlings of this genotype due to alterations in the pigment organization.

In general, however, the POR-independent nature of energy migration between different Pchl(ide) forms suggests the existence of an energy transfer unit with fixed pigment stoichiometries. Thus the spectral shifts seen in the in situ excitation spectra of photoactive Pchlide-F655 (Fig. 6A) probably do not arise from genotype-specific differences in energy transfer between the various Pchl(ide) pigment forms.

Stoichiometries of the Non-Photoactive and Photoactive Pigments within the Pchl(ide) Energy Transfer Unit

To characterize the pigment stoichiometries within such an energy transfer unit the number of non-

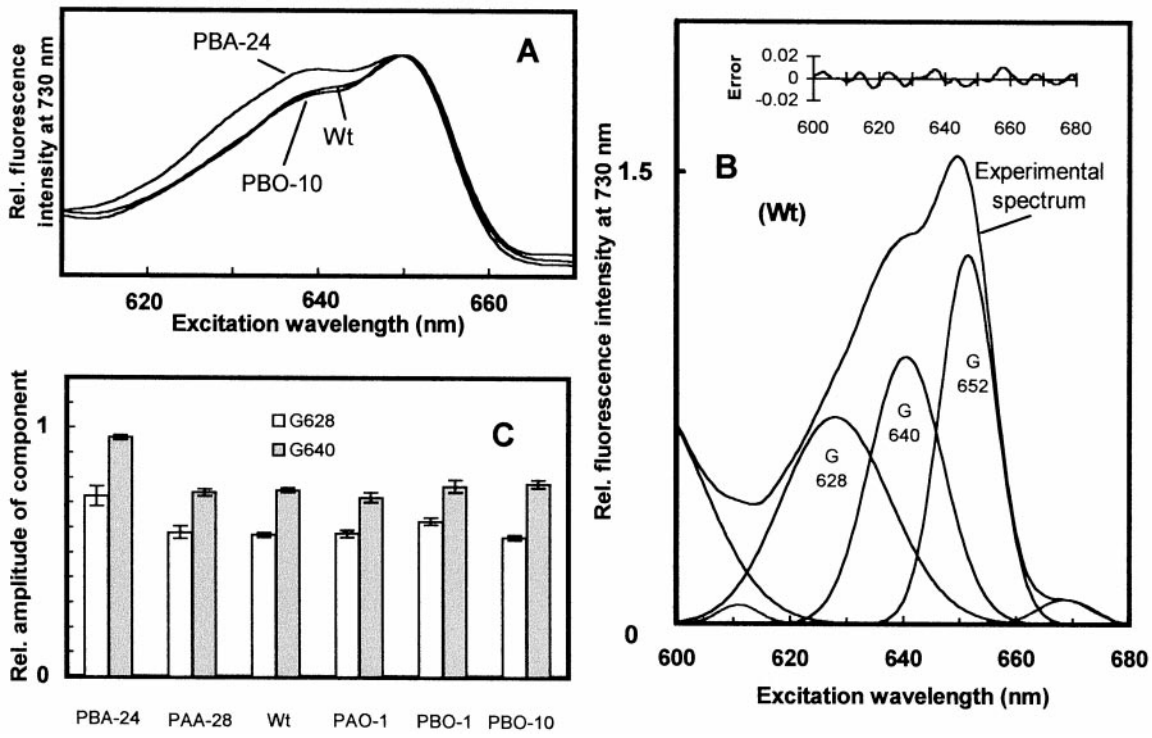

Figure 9. Fluorescence excitation spectra from the red region of photoactive Pchlide-F655 present in situ in etiolated seedlings. A, In situ low temperature excitation spectra of the fluorescence emission at 730 nm, which corresponds to a vibrational sublevel of Pchlide-F655 (Böddi et al., 1992), were collected from cotyledons of 4-d-old wild-type and transgenic seedlings. Spectra were normalized at their respective maxima. B, Gaussian deconvolution of the wild-type excitation spectrum (inset, the difference between the experimental spectrum and the sum of the G628, G640, and G652 gaussian components). C, Relative amplitudes of the G628 and G640 gaussian components (the amplitude of G652 has been defined as 1 for each genotype). Error bars indicate the standard deviations. Seedling genotypes are arranged left to right as POR antisense, wild type, and PORA or PORB overexpressing.

photoactive Pchl(ide) molecules that contribute to the fluorescence emission of a single photoactive Pchlide molecule was calculated (Schoefs et al., 2000). As seen in Figure 10, the ratios of the quantitated amounts of these pigment forms for seedlings with different amounts of total POR were plotted as a function of the ratio of the corresponding low temperature fluorescence emissions at 632 and 655 nm, respectively. The resulting data set was linearly extrapolated to obtain the *y*-intercept, which corresponds to the number of non-photoactive Pchl(ide) molecules that are coupled to a single photoactive Pchlide molecule within an energy transfer unit. The slope of this line depends not only upon the stoichiometries of the pigments involved, but also upon their relative fluorescence yields and extinction coefficients. Data obtained from seedlings of lines PBA-24 and PBO-10 was not included in this analysis because they contain mixtures of DV- and MV-Pchl(ide) that deviate most significantly from that of the wild type (Fig. 8D), which theoretically might influence the ratio of fluorescence emitted in situ at 632 versus 655 nm upon excitation in the Soret region (Fig. 6). Furthermore, line PBA-24 may contain an energy transfer unit with an atypical structure (Fig. 9).

Using data from duplicate measurements of wild-type, PAA-28, PBO-1, and PAO-3 cotyledons, the *y*-intercept was found to have a value of 0.173 (Fig. 10). This corresponds to a non-photoactive Pchl(ide)-to-photoactive Pchlide ratio of 1:6 within an energy transfer unit in the PLB of etiolated Arabidopsis cotyledons. For comparison, the value of the *y*-intercept would decrease to 0.075, corresponding to a pigment ratio of 1:13 if the PBO-10 data point were to be included. Because this ratio is rather sensitive to the distribution of the data points it should be taken primarily as a semiquantitative indication that substoichiometric amounts of non-photoactive pigment are coupled to a large excess of photoactive Pchlide.

Determination of the Kinetics of Photoactive Pchlide Photoreduction in Seedlings

In a final experiment to characterize the pigment-protein complexes of etioplasts we determined the kinetics of photoactive Pchlide reduction in situ at room temperature in cotyledons of wild-type and transgenic seedlings. The approach used was to measure the time course of the increase in Chlide fluo-

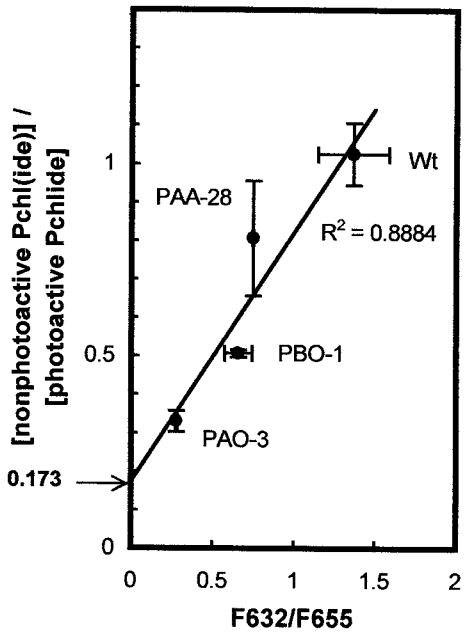

Figure 10. Estimation of the ratio of non-photoactive Pchl(ide)-to-photoactive Pchlide molecules within an energy transfer unit. The ratio of non-photoactive Pchl(ide)-to-photoactive Pchlide obtained from pigment quantitations was plotted against the ratio of the in situ low temperature fluorescence emission bands at 632 and 655 nm for cotyledons of 4-d-old transgenic and wild-type seedlings. A best-fit trendline through the data points was calculated and its correlation coefficient was determined. Error bars indicate the SDS.

rescence during a short (1-s) illumination with intense red light with a maximum at 650 nm.

Actual recordings obtained for cotyledons of the wild type and of lines PBA-24 and PBO-10 are compared in Figure 11A. The fluorescence intensity increased from a low initial value originating from Pchlide vibrational sublevels to a maximum within less than 100 ms under the experimental conditions. On such a short time scale this increase derives exclusively from the formation of the Chlide-F690 photoproduct, with negligible contributions of further Chlide spectral shifts and of photoactive Pchlide regeneration processes (Schoefs et al., 1994; McCormac et al., 1996). The maximal Chlide fluorescence values achieved agree qualitatively with the initial amounts of photoactive Pchlide present (Fig. 4B).

The rate of the fluorescence intensity increase from the initial to the maximum level was used to calculate a halftime for photoactive Pchlide photoreduction under these excitation conditions of 7.0 ms in wild-type seedlings. Halftime values were found to be genotype-dependent with very little variation between repetitions of the same measurement (Fig. 11B). Average halftime values tended to increase, indicating modest decreases in the rates of Pchlide reduction with increasing amounts of photoactive Pchlide (Fig. 4B) and total POR (Fig. 5). Deconvolution of the kinetics into exponential components revealed a biexponential character of the Chlide fluorescence increase in seedlings of all genotypes (data not shown), suggesting no apparent relationship between the amplitudes of the two components and the ratio of PORA to PORB.

DISCUSSION

In Vivo Manipulation of Etioplast Development Suggests Redundant Roles for the Light-Dependent PORA and PORB Enzymes

The two distinguishing features of the etioplast plastid type of dark-grown angiosperms are the accumulation of photoactive Pchlide-F655 and the presence of the PLB inner membrane in which this pigment form is localized (Ryberg and Sundqvist, 1991). These features may reflect the need to efficiently store the pigments and lipids that are later needed for Chl biosynthesis and thylakoid membrane formation during the light-dependent differentiation of etioplasts into chloroplasts. By exploiting the complete range of PORA and PORB expression levels available using antisense and overexpression techniques in Arabidopsis, we have been able to manipulate etioplast development in vivo in a detailed fashion. In

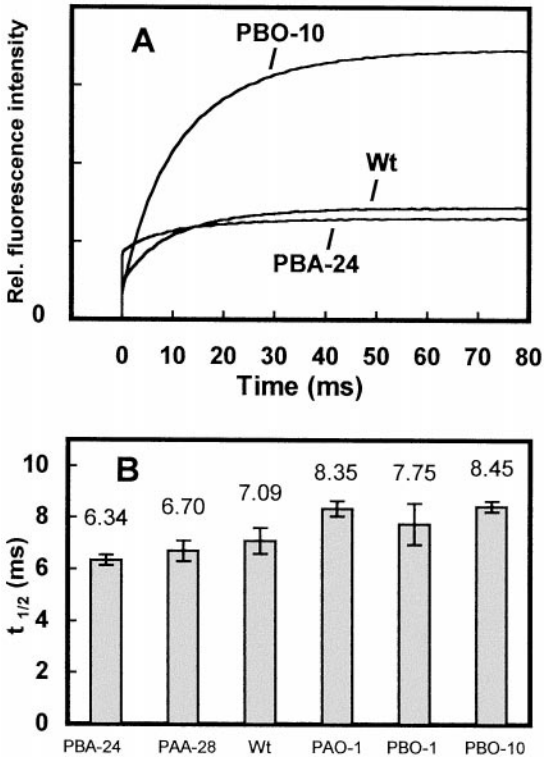

Figure 11. Photoactive Pchlide reduction kinetics upon illumination of etiolated seedlings. A, Time courses of the in situ Chlide fluorescence increase in cotyledons of 4-d-old wild-type and transgenic seedlings exposed to 650 nm light at room temperature. B, Photoactive Pchlide reduction halftimes determined from the rate of the Chlide fluorescence increase. Error bars indicate the standard deviations. Seedling genotypes are arranged left to right as POR antisense, wild type, and PORA- or PORB-overexpressing.

particular, we have examined whether PORA and PORB perform unique functions in etioplasts or whether the properties of this plastid type are determined by total POR content rather than by the ratio of these two enzymes.

As discussed below, increasing total POR content correlates closely with increases in the ratio of PLB-to-PT membranes, the amount of and perturbations in the excitation maxima and photoreduction kinetics of photoactive Pchlide, the ratio of photoactive Pchlide-F655 to non-photoactive Pchl(ide)-F632, and the ratio of DV- to MV-Pchl(ide) *a*. The last result defines POR as the first endogenous protein factor demonstrated to influence the chemical heterogeneity of the Pchl(ide) pool in angiosperms. Excitation energy transfer between different spectroscopic forms of Pchl(ide) present in etiolated cotyledons remains largely POR independent, however. This indicates that Pchl(ide) pigments in the PLB are organized into a minimal structural unit with defined stoichiometries of the various spectroscopically distinguishable forms. Within this unit a small amount of non-photoactive Pchl(ide) transfers its excitation energy to a large excess of photoactive Pchlide-F655. Our data further suggest that POR ternary complexes may bind not only a single molecule of photoactive Pchlide, but also a substoichiometric amount of non-photoactive Pchl(ide), which may correspond to the non-photoactive pigment fraction involved in energy transfer. We conclude that the typical characteristics of etioplasts are closely related to total POR content, rather than to the ratio of PORA-to-PORB.

The Characteristics of Etioplast Pigment-Protein Complexes and Inner Membranes Vary as a Function of Total POR Content

The etioplasts of POR-antisense and POR-overexpressing Arabidopsis seedlings contain a variety of inner membranes architectures ranging from abundant PTs in line PBA-24 to extensive PLBs that monopolize the interior of the organelle in line PBO-10 (Fig. 2). No obvious effects on etioplast inner membrane structure could, however, be specifically attributed to PORA or PORB, as opposed to total POR. Cotyledons of PBA-24 seedlings display an in situ low temperature fluorescence emission spectrum of Pchl(ide) pigment forms dominated by non-photoactive Pchl(ide)-F632 (Fig. 3C). This spectrum strongly resembles that of an isolated PT-enriched membrane fraction obtained from wheat etioplasts (Ryberg and Sundqvist, 1982; Böddi et al., 1989; Ouazzani Chahdi et al., 1998). On the other hand, cotyledons of line PBO-10 exhibit a spectrum with a very prominent photoactive Pchlide-F655 emission (Fig. 3D) that is highly reminiscent of that seen with purified wheat PLB membranes. Therefore, transgenic lines PBA-24 and PBO-10 would be of particular interest for the analysis of different etioplast inner membrane fractions.

Pre- and post-flash low temperature fluorescence emission spectra of etiolated transgenic seedlings containing different amounts of total POR and PORA-to-PORB ratios did not reveal Pchlide or Chlide emission bands specific to only one of the POR enzymes (Fig. 3; Sperling et al., 1998). For example, no PORB-specific emission bands were seen in cotyledons of line PBO-10 (Fig. 3D), which accumulates more than twice as much total POR as the etiolated wild type and represents an extreme phenotype in terms of etioplast membrane structure (Fig. 2B) and pigment levels (Fig. 4). Nevertheless, large genotype-specific variations in the ratio of in situ fluorescence intensities of photoactive Pchlide-F655 to non-photoactive Pchl(ide)-F632 were evident (Fig. 3), and could be confirmed in the quantitative analysis of different Pchl(ide) pigment forms (Fig. 4C). In fact, the amount of photoactive Pchlide present in cotyledons of etiolated Arabidopsis seedlings proved to be directly proportional to total POR content in seedlings, rather than to the ratio of PORA-to-PORB (Fig. 5). More extensive spectroscopic analyses of the Pchl(ide) forms present in POR-overexpressing and POR-antisense seedlings, in particular comparisons of transgenic seedlings with similar levels of total POR (i.e. PAO-1, PAO-3, and PBO-1; Sperling et al., 1998), also did not provide evidence for PORA- or PORB-specific photoactive complexes with distinct biophysical properties (Figs. 6–10). The slightly decreasing rate of photoactive Pchlide photoreduction observed in situ as a function of increasing total POR content (Fig. 11) may be due to indirect effects correlated with the extent of the PLB such as Pchl(ide) pigment screening or changes in light scattering.

Our conclusion that the highly aggregated PORA and PORB photoactive Pchlide-F655 complexes present in vivo in the PLB have very similar, if not identical properties agrees with several other lines of evidence. First, the overexpression of either enzyme in the strongly POR-deficient Arabidopsis *cop1-18* (previously *det340*) mutant leads to the in vivo assembly of the PLB and photoactive Pchlide-F655 (Sperling et al., 1998). Second, a preliminary comparison of the barley PORB and PORA ternary complexes, reconstituted in vitro from bacterially overexpressed MalE::POR fusion proteins, suggests that they too may be biophysically similar (Lebedev and Timko, 1999, and unpublished data cited therein). In this case, the photoactive Pchlide present in the barley complexes displays a blue-shifted low temperature fluorescence emission maximum at 644 rather than 655 nm because of its lower aggregation state, as has been described in other in vitro and in vivo studies (Apel et al., 1980; Ikeuchi and Murakami, 1982; Böddi et al., 1989; Ryberg et al., 1992; Ouazzani Chahdi et al., 1998).

Total POR content is clearly one of the most important factors controlling etioplast differentiation. In the presence of the NADPH and Pchlide needed

to stabilize POR ternary complexes (Ryberg and Sundqvist, 1991), the appropriate combination of lipids required to produce the PLB can be mobilized by PORA or PORB in etiolated Arabidopsis seedlings (Fig. 3; Sperling et al., 1998). That other unidentified factors contribute to the formation of etioplast inner membranes is suggested by the phenotype of the *lip1* constitutive photomorphogenic mutant of pea, an angiosperm that seems to contain only a single *POR* gene (Spano et al., 1992). By analogy to the pleiotropic *cop1* mutant of Arabidopsis (Lebedev et al., 1995; Sperling et al., 1998), *lip1* displays a light-grown seedling morphology even when germinated in the dark and its plastids lack PLBs and normal amounts of photoactive Pchlide-F655 (Seyyedi et al., 1999). However, unlike *cop1*, the *lip1* mutant retains roughly wild-type amounts of POR polypeptide, suggesting that this mutant is defective in some other component(s) required for etioplast differentiation.

POR-Dependent Pchl(ide) *a* Chemical Heterogeneity Influences the in Situ Spectroscopic Properties of Photoactive Pchlide-F655

The in situ low temperature Soret excitation maxima of photoactive Pchlide-F655, and to a much smaller extent of non-photoactive Pchl(ide)-F632, were blue- or red-shifted with respect to the wild type in etiolated cotyledons of Arabidopsis lines PBA-24 and PBO-10, respectively (Figs. 6 and 7). The most likely explanation for these opposing spectral shifts in seedlings containing unusually large or small amounts of POR is provided by our finding that total Pchl(ide) is, in fact, a POR-dependent mixture of DV- and MV-Pchl(ide) (Fig. 8). To the best of our knowledge, no published information about the chemical heterogeneity of Pchl(ide) in Arabidopsis exists. However, the Pchl(ide) *a* present in a number of other angiosperms occurs as a mixture of the DV- and MV-pigments, whose proportions are dependent upon the species, the developmental state, and the growth conditions (Belanger and Rebeiz, 1980; Carey and Rebeiz, 1985; Shioi and Takamiya, 1992; Whyte and Griffiths, 1993; Ioannides et al., 1994). Angiosperms and other higher plants have been classified into several groups according to the ratios of DV-Pchl(ide)-to-MV-Pchl(ide) that they accumulate during photoperiodic growth when harvested in the light versus the dark (Carey and Rebeiz, 1985; Ioannides et al., 1994). The function, if any, of this Pchl(ide) chemical heterogeneity has not been determined. The transgenic POR-overexpressing and POR-antisense Arabidopsis lines described here should therefore provide valuable tools to address this question in vivo.

By analogy to our current study, red shifts have been previously noted in the comparisons of the in situ low temperature excitation maxima of photoactive Pchlide in photoperiodically grown and etiolated bean seedlings (Lebedev et al., 1985), etiolated cucumber and etiolated bean (Cohen and Rebeiz, 1981), greening barley seedlings and etiolated barley seedlings (Franck and Strzalka, 1992), and dark-grown pine and etiolated angiosperms (Schoefs and Franck, 1998). These red shifts likely reflect the relative proportions of DV-Pchl(ide) present in these species under particular growth conditions (Carey and Rebeiz, 1985; Shioi and Takamiya, 1992; Ioannides et al., 1994; Schoefs and Franck, 1998).

Although we consider POR-dependent variations in the relative amounts of photoactive DV- and MV-Pchlide to offer the most likely explanation for the spectral shifts found in the in situ excitation spectra of Pchlide-F655, we cannot entirely exclude several other possibilities. First, in PBO-10 cotyledons the pronounced contributions of the 459 and 472 nm excitation bands might indicate an intrinsically different geometry of the pigment aggregates that fluoresce at 655 nm caused by the unusually high photoactive Pchlide concentration in this transgenic line. Several previous studies have raised the possibility that Pchlide-F655 excitation shoulders at about 460 nm may result from photoactive pigment aggregation (Fradkin et al., 1969; Cohen and Rebeiz, 1981; Ignatov et al., 1983; Böddi et al., 1993). On the other hand, the structure of the Pchl(ide) energy transfer unit in PBO-10 seedlings seems equivalent to that of the wild type (Fig. 9), which would argue against significant aggregation-induced differences in pigment organization. Second, the high amplitudes of the 459 and 472 nm excitation bands might reflect a specific property of the PORB photoactive complex. The red shift in the excitation spectrum of Pchlide-F655 observed during a previous study of the greening process in wild-type barley seedlings (Franck and Strzalka, 1992) could, for example, be interpreted to reflect the expected expression of barley PORB, but not PORA under these conditions (Holtorf et al., 1995a). However, the in situ excitation spectra of Pchlide-F655 in etiolated cotyledons of PAO-3 and PBO-1 seedlings, which overexpress Arabidopsis PORA or PORB to similar extents, are nearly identical (Fig. 7 and data not shown). Furthermore, in vitro studies of reconstituted barley PORB and PORA ternary complexes apparently suggest that these two enzymes have similar properties (Lebedev and Timko, 1999 and unpublished data cited therein).

With respect to the recent hypothesis that non-photoactive Pchl(ide) *b* rather than photoactive Pchl(ide) *a* may be the main pigment species present in etiolated barley seedlings (Reinbothe et al., 1999), we find no spectroscopic evidence that Arabidopsis seedlings contain Pchl(ide) *b* (Fig. 8A and data not shown). Furthermore, most of the Pchl(ide) *a* present in etiolated cotyledons is photoactive (Fig. 4). These results are in accordance with other studies of higher plants, including barley (Granick and Gassman, 1970; Adra and Rebeiz, 1998; Scheumann et al., 1999; Seyyedi et al., 1999) and support the consensus view that etiolated angiosperms contain exclusively

Pchl(ide) *a*, most of which is photoactive (Armstrong et al., 2000).

Substrate Competition between POR and DV-Pchl(ide) Reductase May Regulate Pchl(ide) *a* Chemical Heterogeneity in Angiosperms

Prior to the work reported here, the endogenous factors responsible for the wide range of DV-Pchl(ide)-to-MV-Pchl(ide) *a* pigment ratios observed in various etiolated and photoperiodically grown angiosperms had been the subject of speculation. It had, for example, been proposed that Pchl(ide) *a* chemical heterogeneity might reflect the activity of the putative DV-Pchl(ide) reductase, an enzyme postulated to convert DV- to MV-Pchl(ide) by reduction of the 8-vinyl group and/or the availability of reducing equivalents for this enzyme (Griffiths, 1991; Whyte and Griffiths, 1993; Suzuki and Bauer, 1995; Kim et al., 1997).

Our observation that the proportions of DV-Pchl(ide) in the total Pchl(ide) and photoactive Pchlide pools increase as a function of POR content (Figs. 5 and 8D) raises the question of the mechanism. In fact POR can use DV- or MV-Pchlide *a* as a substrate in vitro in reconstituted ternary complexes and in vivo in intact cotyledons and seems to bind both pigments with roughly similar affinities (Fig. 8D; Griffiths, 1991; Knaust et al., 1993; Whyte and Griffiths, 1993; Adra and Rebeiz, 1998). Although POR might conceivably compete with the putative DV reductase for NADPH binding, it has been argued that the amount of this cofactor does not limit the activities of these enzymes in plastids (Griffiths, 1991; Kim et al., 1997). Rather, we propose that PORA and PORB compete with the DV reductase for the binding of newly synthesized DV Pchl(ide) *a* and that this competition together with the relative catalytic activities of these enzymes generates the Pchl(ide) chemical heterogeneity observed in vivo. In etiolated seedlings the amount of photoactive DV-Pchlide sequestered in dark-stable POR ternary complexes and hence presumably inaccessible to the DV reductase would therefore increase as a function of total POR content.

Photoactive Pchlide-F655 and POR Occur in a 1:1 Stoichiometry in Vivo

The direct proportionality between the amount of photoactive Pchlide and total POR content (Fig. 5) indicates a defined pigment-to-protein stoichiometry in the various Arabidopsis lines investigated and suggests that PORA and PORB bind the same number of enzymatically active pigment molecules. Several early in vitro studies reported stoichiometries between the Pchlide pigment and POR polypeptide ranging from 1:1 to 3:1 (Apel et al., 1980; Ikeuchi and Murakami, 1982; Ryberg and Sundqvist, 1982). A 1:1 ratio of photoactive Pchlide to POR is supported by recent data obtained in vitro by reconstituting a barley PORB fusion protein (Lebedev and Timko, 1999) and with a highly purified POR preparation from oat PLBs (Klement et al., 1999).

That a 1:1 ratio of photoactive pigment-to-POR protein occurs in vivo can also be concluded from the fact that in most plants including Arabidopsis (Fig. 4C), photoactive Pchlide is the main pigment form in mature etioplasts in situ (Granick and Gassman, 1970; Adra and Rebeiz, 1998; Seyyedi et al., 1999). Taking into account that POR possesses a single NADPH-binding site, each dark-stable ternary complex should reduce only one photoactive Pchlide molecule per light flash. It seems highly unlikely that the $NADP^+$ generated by the flash-induced photoreduction of a single molecule of photoactive Pchlide at the POR active site could exchange freely with the environment or be rereduced in situ during 1 ms at −20°C. The simplest explanation for the result that most of the total Pchl(ide) in cotyledons of etiolated seedlings is photoactive is therefore the existence of a 1:1:1 stoichiometry of photoactive Pchlide-to-NADPH-to-POR in the ternary complexes.

Pchl(ide) Pigment Forms Exist in Structurally Conserved Energy Transfer Units within Etioplast Inner Membranes

Previous spectroscopic studies have demonstrated that excitation energy migrates from short-wavelength Pchlide forms [i.e. non-photoactive Pchl(ide)-F632 and photoactive Pchlide-F645] to photoactive Pchlide-F655 (Kahn et al., 1970; Sironval and Brouers, 1970; Ignatov et al., 1983). One might therefore expect different relative contributions of short-wavelength Pchl(ide) excitation bands to the excitation spectra of Pchlide-F655 in plants with different photoactive-to-non-photoactive pigment ratios. This would, in principle, apply to the red and Soret regions, although in the latter case the assignment of the excitation bands to specific Pchl(ide) forms is more difficult. Nevertheless, despite substantial variations in the photoactive-to-non-photoactive pigment ratio in cotyledons of seedlings of different genotypes (Fig. 4C), we found in all but one case unaltered contributions of the Pchl(ide)-F632 and Pchlide-F645 excitation bands at 628 and 640 nm, respectively, to the in situ fluorescence emission of Pchlide-F655 (Fig. 9, B and C).

These results suggest the occurrence of a structure or energy transfer unit within the PLB in which different Pchlide forms are associated in constant proportions that are independent of the relative amounts of PORA and PORB and the total POR content. Within such a structure a small amount of non-photoactive Pchl(ide) transfers its excitation energy to a large excess of photoactive Pchlide (Fig. 10). POR overexpression in seedlings of line PBO-10 led to a large change in the proportions of photoactive DV-

Pchlide and non-photoactive DV-Pchl(ide) (Fig. 8D), but had no apparent effect on the spectroscopic properties of the energy transfer unit (Fig. 9A). Thus this structure seems to be insensitive to the chemical heterogeneity of the endogenous Pchl(ide) pool and to the local concentration of photoactive Pchlide-F655 in the etioplast.

In line PBA-24, in contrast to seedlings of other genotypes, the in situ excitation spectrum of Pchlide-F655 in the red region differed in that the relative amplitudes of the Pchl(ide)-F632 and Pchlide-F645 bands at 628 and 640 nm, respectively, were significantly higher. This indicates that the Pchlide energy transfer units contain unusually high ratios of short-wavelength Pchlide forms, in agreement with the low ratio of photoactive-to-non-photoactive pigment measured quantitatively (Fig. 4C) and consistent with the unusually high ratio of PT-to-PLB inner membranes visible in electron micrographs of PBA-24 etioplasts (Fig. 2C).

To reconcile the existence of an energy transfer unit with fixed stoichiometries of the different Pchl(ide) pigment forms with the various ratios of photoactive Pchlide-to-non-photoactive Pchl(ide) observed in vivo (Fig. 4C), one must postulate the existence of a pool of non-photoactive Pchl(ide)-F632 that does not participate in energy transfer. Recent spectroscopic measurements of different developmental stages of etiolated bean leaves have led to a similar conclusion (Schoefs et al., 2000). Because energy transfer units containing Pchlide-F655, Pchlide-F645 and Pchl(ide)-F632 in fixed ratios are expected to be concentrated in PLBs, excess Pchl(ide)-F632 may be localized primarily in PTs and hence spatially separated from aggregated POR ternary complexes. In support of this model, previous studies with wheat etioplast inner membrane fractions have demonstrated the ratio of non-photoactive Pchl(ide)-F632-to-photoactive Pchlide-F655 to be much higher in PTs than in PLBs (Ryberg and Sundqvist, 1982; Böddi et al., 1989; Ouazzani Chahdi et al., 1998). We have also found strong qualitative correlations between the amount of photoactive Pchlide and the extent of the PLB and the amount of non-photoactive Pchl(ide) and the occurrence of the PTs (Figs. 2 and 4; Sperling et al., 1998). A further possibility is that some of the Pchl(ide)-F632 located outside of energy transfer units might be found in etioplast envelope membranes. Spinach chloroplast envelope membranes, for example, do contain a small amount of Pchl(ide)-F632, although it was not reported whether this pigment was non-photoactive upon flash illumination (Joyard et al., 1990).

POR May Bind Substoichiometric Amounts of Non-Photoactive Pchlide That Transfer Excitation Energy to Photoactive Pchlide

It is interesting that the POR-dependent increase in the relative amount of DV-Pchl(ide) as a fraction of total Pchl(ide) holds true not only for the POR-bound photoactive pigment, but also for non-photoactive Pchl(ide) (Fig. 8D). This result is difficult to understand if one considers all of the non-photoactive DV-Pchl(ide) molecules to be "free," and hence readily accessible to the putative DV reductase rather than to be at least partially sequestered. One possible explanation consistent with our data is that POR binds not only a stoichiometric amount of photoactive Pchlide at the active site, but also a substoichiometric amount of non-photoactive Pchlide at a second site. The existence of such a second site is supported by reconstitution studies of oat POR by Klement et al. (1999). If non-photoactive Pchlide were to be bound to this site it would be in close proximity to photoactive Pchlide, which would explain that energy transfer from a subpopulation of Pchl(ide)-F632 to Pchlide-F655 takes place within the PLB (Fig. 10).

MATERIALS AND METHODS

Plasmid Constructs

Plasmid vectors suitable for the antisense inhibition of expression of PORA and PORB in Arabidopsis were prepared, propagated in *Escherichia coli*, and analyzed according to standard procedures (Sambrook et al., 1989). pPORA1.0 and pPORB1.0, which carry the complete coding regions of the Arabidopsis *PORA* and *PORB* cDNAs, respectively (Armstrong et al., 1995), were modified by the insertion of an oligonucleotide containing an internal *Eco*RI restriction site (5′-TCGAGAATTC-3′) into their unique *Sal*I sites. The *POR* cDNAs were then excised as *Eco*RI fragments and thereafter ligated into pSH9 3′ to the cauliflower mosaic virus 35 S promoter fused to the omega translational enhancer (Holtorf et al., 1995b). pSH9 derivatives containing the *POR* cDNAs in the antisense orientation with respect to the promoter were identified and the expression cassettes excised by partial digestion with *Hin*dIII. These fragments were then ligated into the pBIN19 binary vector (Bevan, 1984). The resulting plasmids, p35SΩ::PORA2.0AS and p35SΩ::PORB2.0AS, were introduced into *Agrobacterium tumefaciens* strain C58C1rif (pGV3850).

Plant Transformation and Growth Conditions

Transgenic Arabidopsis plants of the ecotype Columbia derivative C24 were produced by incubation of *A. tumefaciens* strains containing p35SΩ::PORA2.0AS or p35SΩ::PORB2.0AS with excised roots and subsequent regeneration of putatively transformed T_1 shoots from calli (Valvekens et al., 1988). Transgenic T_1 shoots were selected on kanamycin-containing (50 μg/mL) Murashige-Skoog agar Petri plates. Of the initial T_1 transformants, 11 PAA and five PBA lines were propagated and their T_2 progenies were examined by selection on kanamycin-containing medium. Further propagation of multiple T_2 plants from each line allowed the identification of homozygous plants from seven PAA and three PBA T_1 lines based on kanamycin resistance segregation ratios among the T_3 progenies.

Southern-blot analyses to determine the genomic organization of the transgenes revealed six out of seven PAA and all three PBA lines to have originated from independent transformation events (data not shown). The generation and some phenotypic properties of homozygous transgenic Arabidopsis plants that overexpress PORA (lines PAO-1 and PAO-3) or PORB (lines PBO-1 and PBO-10) have been previously described (Sperling et al., 1997, 1998, 1999). Etiolated seedlings of all genotypes were obtained by sowing surface-sterilized seeds on Murashige-Skoog agar plates, which were subsequently placed in the dark at 4°C for 24 h, exposed at 22°C to 1 h of white light at a fluence rate of 160 μE m^{-2} s^{-1} provided by TLD 36W/84 cool-white fluorescent lamps (Philips, Eindhoven, The Netherlands), and thereafter returned to darkness at room temperature for 4 d. Plant material was harvested under a green safety light and processed immediately for electron microscopy and spectroscopic measurements or frozen in liquid nitrogen and stored at −80°C until further analysis of the RNA and protein contents.

mRNA, Protein, and Plastid Ultrastructural Analyses

Whole etiolated Arabidopsis seedlings were harvested for gel-blot analyses of their mRNA and protein contents, whereas cotyledons were collected for plastid ultrastructural analysis by transmission electron microscopy. Plant material was handled and quantitative data was obtained as previously described (Armstrong et al., 1995; Sperling et al., 1997, 1998). The amounts of the mRNAs for *PORA*, *PORB*, and the actin (*ACT*) gene family were determined by hybridization of radioactively labeled Arabidopsis DNA probes with gel blots containing total RNA. Total POR protein content was determined using a polyclonal anti-Arabidopsis POR antiserum.

In Situ Low Temperature Fluorescence Spectroscopy

Pre-flash and post-flash low temperature fluorescence emission spectra of three pairs of cotyledons from etiolated seedlings were recorded at an excitation wavelength of 440 nm using an LS50 or LS50B luminescence spectrophotometer (Perkin-Elmer, Foster City, CA), as described below and in Sperling et al. (1998). Excitation and emission slits were set to 10 and 5 nm, respectively. The temperature recorded during the measurements of cotyledons maintained in liquid nitrogen varied between 83 and 93 K. For post-flash spectra, a 1-ms light pulse from a photographic flash attachment was used to convert photoactive Pchlide to Chlide after allowing the sample to warm up to −20°C (Sironval and Brouers, 1970). The spectra were corrected for the baseline and the photomultiplier sensitivity. For measurements of emission spectra and of excitation spectra in the Soret region, a low-pass blue filter ($\lambda < 580$ nm) was placed in front of the excitation window and a high-pass red filter ($\lambda > 600$ nm) was placed in front of the emission window to minimize stray light. For measurements of excitation spectra in the red region, the blue filter was removed and the 600-nm filter was replaced by a high-pass red filter ($\lambda > 725$ nm). Excitation spectra were corrected for the baseline and for the spectrum of the xenon lamp.

Quantitative Measurements of Pigment Content by in Vitro Room and Low Temperature Fluorescence Spectroscopy

Room temperature fluorescence emission and excitation analyses of the Pchl(ide) and Chlide present in etiolated seedlings before and after flash treatment were performed using total pigments extracted from three pairs of cotyledons with 1 mL of 80% aqueous acetone. Emission spectra of the pigment extracts were recorded with the LS50 spectrophotometer set at an excitation wavelength of 435 nm and the excitation and emission slit widths set at 10 and 5 nm, respectively. Measurements were repeated two or three times using independent sets of cotyledons. The total Pchl(ide) and photoactive Pchlide pigment contents were then calculated as described in Sperling et al. (1998). Room temperature excitation spectra of the total Pchl(ide) fluorescence emission band at 634 nm were recorded using excitation and emission slit widths of 5 and 10 nm, respectively. Ratios of DV-Pchl(ide)-to-MV-Pchl(ide) were assessed by the method of Tripathy and Rebeiz (1985) based on analysis of low temperature fluorescence excitation spectra of extracted pigments in diethyl ether. Ten pairs of cotyledons were first extracted with 80% aqueous acetone and total Pchl(ide) was quantitated as described above. After transfer of the Pchl(ide) to an equal volume of diethyl ether, pigment samples were frozen at 77 K in 2-mm diameter glass tubes. Excitation spectra of the Pchl(ide) fluorescence emission band at 625 nm were recorded between 400 and 500 nm using a narrow excitation slit width of 2.5 nm and an emission slit width of 5 nm. After correction of the spectra for the baseline, the DV-Pchl(ide)-to-MV-Pchl(ide) fluorescence ratios were calculated according to equations 15 and 16 in Tripathy and Rebeiz (1985) and converted to concentration ratios as indicated therein. These analyses were performed with etiolated and flash-treated seedlings to determine the DV-Pchl(ide)-to-MV-pigment ratios within the photoactive Pchlide and non-photoactive Pchl(ide) fractions.

Excitation Spectrum Analysis by Gaussian Deconvolution

Resolution of the in situ low temperature fluorescence excitation spectra into gaussian components was performed using the SPSERV program (Bagyinka, 1984; Böddi et al., 1992). A five-point linear smoothing function was repeated 100 times to decrease the noise. Approximate positions of the excitation components were then obtained from the fourth derivative of the smoothed spectra. These positions were used as initial values for gaussian analysis. Resolutions were then repeated several times, with the bandwidth and the wavelength maximum of each component alternately allowed to vary for optimization during the curve fitting until the error level was less than 1% of the signal.

Photoactive Pchlide Reduction Kinetics

Kinetic measurements of Pchlide photoreduction in etiolated cotyledons were determined from fluorescence data collected in situ at room temperature using a Plant Efficiency Analyzer (Hansatech, King's Lynn, UK). The exciting light was provided by light-emitting diodes with an emission maximum at 650 nm (one-half-bandwidth, 25 nm). Chlide fluorescence detected through a high-pass red filter (50% transmission at 720 nm) was measured from its first vibrational sublevel at approximately 745 to 750 nm (Fig. 3). Photoactive Pchlide contributes negligibly to this signal because its fluorescence yield at room temperature is much lower than that of the initial Chlide-F690 photoreduction product (Eullaffroy et al., 1998). Thus the photoreduction of photoactive Pchlide to Chlide causes a large increase in the fluorescence emission intensity at wavelengths greater than 720 nm.

ACKNOWLEDGMENTS

We would like to thank Béla Böddi for valuable discussions and Dieter Rubli for photography.

Received May 5, 2000; modified July 31, 2000; accepted September 19, 2000.

LITERATURE CITED

Adra AN, Rebeiz CA (1998) Chloroplast biogenesis 81: transient formation of divinyl chlorophyll *a* following a 2.5 ms light flash treatment of etiolated cucumber cotyledons. Photochem Photobiol **68:** 852–856

Apel K, Santel H-J, Redlinger TE, Falk H (1980) The protochlorophyllide holochrome of barley (*Hordeum vulgare* L.): isolation and characterization of the NADPH-protochlorophyllide oxidoreductase. Eur J Biochem **111:** 251–258

Armstrong GA, Apel K, Rüdiger W (2000) Does a light-harvesting protochlorophyllide *a/b*-binding protein complex exist? Trends Plant Sci **5:** 40–44

Armstrong GA, Runge S, Frick G, Sperling U, Apel K (1995) Identification of NADPH:protochlorophyllide oxidoreductases A and B: a branched pathway for light-dependent chlorophyll biosynthesis in *Arabidopsis thaliana*. Plant Physiol **108:** 1505–1517

Bagyinka C, copyrighter (1984) SPSERV program. Biological Research Center of the Hungarian Academy of Sciences, Szeged, Hungary

Beale SI (1999) Enzymes of chlorophyll biosynthesis. Photosynthesis Res **60:** 43–73

Belanger FC, Rebeiz CA (1980) Chloroplast biogenesis: detection of divinyl protochlorophyllide in higher plants. J Biol Chem **255:** 1266–1272

Bevan M (1984) Binary *Agrobacterium* vectors for plant transformation. Nucleic Acids Res **12:** 8711–8721

Böddi B, Lindsten A, Ryberg M, Sundqvist C (1989) On the aggregational states of protochlorophyllide and its protein complexes in wheat etioplasts. Physiol Plant **76:** 135–143

Böddi B, Ryberg M, Sundqvist C (1992) Identification of four universal protochlorophyllide forms in dark-grown leaves by analyses of the 77 K fluorescence emission spectra. J Photochem Photobiol B Biol **12:** 389–401

Böddi B, Ryberg M, Sundqvist C (1993) Analysis of the 77 K fluorescence emission and excitation spectra of isolated etioplast inner membranes. J Photochem Photobiol B Biol **21:** 125–133

Carey EE, Rebeiz CA (1985) Chloroplast biogenesis 49: differences among angiosperms in the biosynthesis and accumulation of monovinyl and divinyl protochlorophyllide during photoperiodic greening. Plant Physiol **79:** 1–6

Cohen CE, Rebeiz CA (1981) Chloroplast biogenesis 34: spectral fluorometric characterization *in situ* of the protochlorophyll species in etiolated tissues of higher plants. Plant Physiol **67:** 98–103

Eullaffroy P, Popovic R, Franck F (1998) Changes of chlorophyll(ide) fluorescence yield induced by a short light pulse as a probe to monitor the early steps of etioplast phototransformation in dark-grown leaves. Photochem Photobiol **67:** 676–682

Fradkin LI, Shlyk AA, Kalina LM, Faludi-Dániel Á (1969) Fluorescence studies on the reaction centers of chlorophyll biosynthesis in the early stages of greening. Photosynthetica **3:** 326–337

Franck F, Strzalka K (1992) Detection of the photoactive protochlorophyllide-protein complex in the light during the greening of barley. FEBS Lett **309:** 73–77

Granick S, Gassman M (1970) Rapid regeneration of protochlorophyllide$_{650}$. Plant Physiol **45:** 201–205

Griffiths WT (1978) Reconstitution of chlorophyllide formation by isolated etioplast membranes. Biochem J **174:** 681–692

Griffiths WT (1991) Protochlorophyllide photoreduction. *In* H Scheer, ed, Chlorophylls. CRC Press, Boca Raton, FL, pp 433–449

Holtorf H, Reinbothe S, Reinbothe C, Bereza B, Apel K (1995a) Two routes of chlorophyllide synthesis that are differentially regulated by light in barley. Proc Natl Acad Sci USA **92:** 3254–3258

Holtorf S, Apel K, Bohlmann H (1995b) Comparison of different constitutive and inducible promoters for the overexpression of transgenes in *Arabidopsis thaliana*. Plant Mol Biol **29:** 637–646

Ignatov NV, Krasnovskiĭ AA Jr, Litvin FF, Belyaeva O, Walter G (1983) Low-temperature (77 K) excitation spectra of fluorescence and phosphorescence of native forms of protochlorophyll(ide) in etiolated leaves of *Phaseolus vulgaris* and *P. coccineus*. Photosynthetica **17:** 352–360

Ikeuchi M, Murakami S (1982) Measurement and identification of NADPH:protochlorophyllide oxidoreductase solubilized with Triton X-100 from etioplast membranes of squash cotyledons. Plant Cell Physiol **23:** 1089–1099

Ioannides IM, Fasoula DA, Robertson KR, Rebeiz CA (1994) An evolutionary study of chlorophyll biosynthetic heterogeneity in green plants. Biochem System Ecol **22:** 211–220

Joyard J, Block M, Pineau B, Albrieux C, Douce R (1990) Envelope membranes from mature spinach chloroplasts contain a NADPH:protochlorophyllide reductase on the cytosolic side of the outer membrane. J Biol Chem **265:** 21820–21827

Kahn A, Boardman NK, Thorne SW (1970) Energy transfer between protochlorophyllide molecules: evidence for multiple chromophores in the photoactive protochlorophyllide-protein complex *in vivo* and *in vitro*. J Mol Biol **48:** 85–101

Kim JS, Kolossov V, Rebeiz CA (1997) Chloroplast biogenesis 76: regulation of 4-vinyl reduction during conversion of divinyl Mg-protoporphyrin IX to monovinyl protochlorophyllide *a* is controlled by plastid membrane and stromal factors. Photosynthetica **34:** 569–581

Klement H, Helfrich M, Oster U, Schoch S, Rüdiger W (1999) Pigment-free NADPH:protochlorophyllide oxidoreductase from *Avena sativa* L.: purification and substrate specificity. Eur J Biochem **265:** 862–874

Knaust R, Seyfried B, Schmidt L, Schulz R, Senger H (1993) Phototransformation of monovinyl and divinyl protochlorophyllide by NADPH:protochlorophyllide oxidoreductase of barley expressed in *Escherichia coli*. J Photochem Photobiol B Biol **20:** 161–166

Kümmel HW, Grimme LH (1974) The inhibition of carotenoid biosynthesis in green algae by SANDOZ H6706: accumulation of phytoene and phytofluene in *Chlorella fusca*. Z Naturforsch **30c:** 333–336

Lebedev N, Timko MP (1999) Protochlorophyllide oxidoreductase B-catalyzed protochlorophyllide photoreduction *in vitro*: insight into the mechanism of chlorophyll formation in light-adapted plants. Proc Natl Acad Sci USA **96:** 9954–9959

Lebedev N, van Cleve B, Armstrong G, Apel K (1995) Chlorophyll synthesis in a de-etiolated (det340) mutant of *Arabidopsis* without NADPH-protochlorophyllide (PChlide) oxidoreductase (POR) A and photoactive PChlide-F655. Plant Cell **7:** 2081–2090

Lebedev NN, Siffel P, Krasnovskii AA (1985) Detection of protochlorophyllide forms in irradiated green leaves and chloroplasts by difference fluorescence spectroscopy at 77 K. Photosynthetica **19:** 183–187

McCormac DJ, Marwood CA, Bruce D, Greenberg BM (1996) Assembly of photosystem I and II during the early phases of light-induced development of chloroplasts from proplastids in *Spirodela oligorrhiza*. Photochem Photobiol **63:** 837–845

Ouazzani Chahdi MAO, Schoefs B, Franck F (1998) Isolation and characterization of photoactive complexes of NADPH:protochlorophyllide oxidoreductase from wheat. Planta **206:** 673–680

Reinbothe C, Lebedev N, Reinbothe S (1999) A protochlorophyllide light-harvesting complex involved in de-etiolation of higher plants. Nature **397:** 80–84

Reinbothe S, Reinbothe C, Lebedev N, Apel K (1996) PORA and PORB, two light-dependent protochlorophyllide-reducing enzymes of angiosperm chlorophyll biosynthesis. Plant Cell **8:** 763–769

Runge S, Sperling U, Frick G, Apel K, Armstrong GA (1996) Distinct roles for light-dependent NADPH:protochlorophyllide oxidoreductases (POR) A and B during greening in higher plants. Plant J **9:** 513–523

Ryberg M, Artus N, Böddi B, Lindsten A, Wiktorsson B, Sundqvist C (1992) Pigment-protein complexes of chlorophyll precursors. *In* JH Argyroudi-Akoyunoglou, ed, Regulation of Chloroplast Biogenesis. Plenum Press, New York, pp 217–224

Ryberg M, Sundqvist C (1982) Characterization of prolamellar bodies and prothylakoids fractionated from wheat etioplasts. Physiol Plant **56:** 125–132

Ryberg M, Sundqvist C (1991) Structural and functional significance of pigment-protein complexes of chlorophyll precursors. *In* H Scheer, ed, Chlorophylls. CRC Press, Boca Raton, FL, pp 587–612

Sambrook J, Fritsch EF, Maniatis T (1989) Molecular Cloning: A Laboratory Manual, Ed 2. Cold Spring Harbor Laboratory Press, Cold Spring Harbor, NY

Scheumann V, Klement H, Helfrich M, Oster U, Schoch S, Rüdiger W (1999) Protochlorophyllide *b* does not occur in barley etioplasts. FEBS Lett **445:** 445–448

Schoch S, Helfrich M, Wiktorsson B, Sundqvist C, Rüdiger W, Ryberg M (1995) Photoreduction of zinc protopheophorbide *b* with NADPH-protochlorophyllide oxidoreductase from etiolated wheat (*Triticum aestivum L.*). Eur J Biochem **229:** 291–298

Schoefs B, Bertrand M, Franck F (2000) Spectroscopic properties of protochlorophyll(ide) analyzed *in situ* in the course of etiolation and in illuminated leaves. Photochem Photobiol **72:** 85–93

Schoefs B, Franck F (1998) Chlorophyll synthesis in dark-grown pine primary needles. Plant Physiol **118:** 1159–1168

Schoefs B, Garnir HP, Bertrand M (1994) Comparison of the photoreduction of protochlorophyllide to chlorophyllide in leaves and cotyledons from dark-grown bean as a function of age. Photosynth Res **41:** 405–417

Seyyedi M, Timko MP, Sundqvist C (1999) Protochlorophyllide, NADPH-protochlorophyllide oxidoreductase, and chlorophyll formation in the *lip1* mutant of pea. Physiol Plant **106:** 344–354

Shioi Y, Takamiya KI (1992) Monovinyl and divinyl protochlorophyllide pools in etiolated tissues of higher plants. Plant Physiol **100:** 1291–1295

Sironval C, Brouers M (1970) The reduction of protochlorophyllide into chlorophyllide: II. The temperature dependence of the $P_{657-647} \rightarrow P_{688-676}$ phototransformation. Photosynthetica **4:** 38–47

Spano AJ, He Z, Michel H, Hunt DF, Timko MP (1992) Molecular cloning, nuclear gene structure, and developmental expression of NADPH:protochlorophyllide oxidoreductase in pea (*Pisum sativum* L.). Plant Mol Biol **18:** 967–972

Sperling U, Franck F, van Cleve B, Frick G, Apel K, Armstrong GA (1998) Etioplast differentiation in Arabidopsis: both PORA and PORB restore the prolamellar body membrane and photoactive protochlorophyllide-F655 to the *cop1* photomorphogenic mutant. Plant Cell **10:** 283–296

Sperling U, Frick G, van Cleve B, Apel K, Armstrong GA (1999) Pigment-protein complexes, plastid development and photooxidative protection: the effects of PORA

and PORB overexpression on *Arabidopsis* seedlings shifted from far-red to white light. *In* JH Argyroudi-Akoyunoglou and H Senger, eds, The Chloroplast: From Molecular Biology to Biotechnology. Kluwer Academic Publishers, Dordrecht, The Netherlands, pp 97–102

Sperling U, van Cleve B, Frick G, Apel K, Armstrong GA (1997) Overexpression of light-dependent PORA or PORB in plants depleted of endogenous POR by far-red light enhances seedling survival in white light and protects against photooxidative damage. Plant J **12:** 649–658

Suzuki JY, Bauer CE (1995) Altered monovinyl and divinyl protochlorophyllide pools in *bchJ* mutants of *Rhodobacter capsulatus*. J Biol Chem **270:** 3732–3740

Tripathy BC, Rebeiz CA (1985) Chloroplast biogenesis: quantitative determination of monovinyl and divinyl Mg-protoporphyrins and protochlorophyll(ides) by spectrofluorometry. Anal Biochem **149:** 43–61

Valvekens D, van Montagu M, van Lijsebettens M (1988) *Agrobacterium tumefaciens*-mediated transformation of *Arabidopsis thaliana* root explants by using kanamycin selection. Proc Natl Acad Sci USA **85:** 5536–5540

Virgin H (1981) The physical state of protochlorophyll(ide) in plants. Annu Rev Plant Physiol **32:** 451–463

Whyte BJ, Griffiths WT (1993) 8-Vinyl reduction and chlorophyll *a* biosynthesis in higher plants. Biochem J **291:** 939–944